A Highly Temperature-sensitive Proton Current in Mouse Bone Marrow–derived Mast Cells

Miyuki Kuno, Junko Kawawaki, and Fusao Nakamura

From the Department of Physiology, Osaka City University Medical School, Abeno-ku, Osaka 545, Japan

ABSTRACT Proton (H^+) conductive pathways are suggested to play roles in the regulation of intracellular pH. We characterized temperature-sensitive whole cell currents in mouse bone marrow–derived mast cells (BMMC), immature proliferating mast cells generated by in vitro culture. Heating from 24 to 36°C reversibly and repeatedly activated a voltage-dependent outward conductance with Q_{10} of 9.9 ± 3.1 (mean ± SD) ($n = 6$). Either a decrease in intracellular pH or an increase in extracellular pH enhanced the amplitude and shifted the activation voltage to more negative potentials. With acidic intracellular solutions (pH 5.5), the outward current was detected in some cells at 24°C and Q_{10} was 6.0 ± 2.6 ($n = 9$). The reversal potential was unaffected by changes in concentrations of major ionic constituents (K^+, Cl^-, and Na^+), but depended on the pH gradient, suggesting that H^+ (equivalents) is a major ion species carrying the current. The H^+ current was featured by slow activation kinetics upon membrane depolarization, and the activation time course was accelerated by increases in depolarization, elevating temperature and extracellular alkalization. The current was recorded even when ATP was removed from the intracellular solution, but the mean amplitude was smaller than that in the presence of ATP. The H^+ current was reversibly inhibited by Zn^{2+} but not by bafilomycin A_1, an inhibitor for a vacuolar type H^+-ATPase. Macroscopic measurements of pH using a fluorescent dye (BCECF) revealed that a rapid recovery of intracellular pH from acid-load was attenuated by lowering temperature, addition of Zn^{2+}, and depletion of extracellular K^+, but not by bafilomycin A_1. These results suggest that the H^+ conductive pathway contributes to intracellular pH homeostasis of BMMC and that the high activation energy may be involved in enhancement of the H^+ conductance.

KEY WORDS: H^+ conductive pathway • pH regulation • temperature • ATP • recovery from acid-load

INTRODUCTION

The importance of intracellular pH (pH_i)[1] regulation is unquestionable in various cellular functions, and the pH_i regulatory mechanisms vary considerably among different types of cells (Hoffmann and Simonsen, 1989). Recently voltage-activated H^+ currents were found in certain cell types of hematopoietic (DeCoursey and Cherny, 1993; Demaurex et al., 1993; Kapus et al., 1993; Holevinsky et al., 1994; Nordström et al., 1995) and nonhematopoietic origin (Thomas and Meech, 1982; Byerly et al., 1984; DeCoursey, 1991; Krause et al., 1993). The H^+ conductive pathway is considered to contribute significantly to pH_i homeostasis, as well as ion exchangers, H^+ pumps and ion cotransporters. However, permeation mechanisms of the H^+ conductance remain to be proved, and the putative H^+ channel is suggested to be different from the general water-filled ion channels (DeCoursey and Cherny, 1995).

Bone marrow–derived mast cells (BMMC) are immature, proliferating mast cells differentiated from multipotential hematopoietic stem cells of bone marrow by in vitro culture in the presence of mast cell growth factors (Ihle et al., 1983; Razin et al., 1984). These cells have characteristics of mast cells, secreting histamine and other chemical mediators upon antigenic stimulation, and also have the potency to differentiate into the different peripheral phenotypes (Nakano et al., 1985). BMMC offer an excellent model to study roles of ion channels in different functional and developmental states. We recently reported that electrophysiological properties of BMMC were heterogeneous (Kuno et al., 1995*a*) but could not identify H^+ conductance. These recordings were made at room temperature, however, and a functional significance of the membrane conductances should be evaluated at physiological temperature.

The present data provide evidence for the presence of a H^+ conductive pathway in BMMC. The H^+ conductance shares common electrophysiological features with those in other cell types (voltage- and time-dependent activation, sensitivity to both pH_i and pH_o and blockage by heavy metals) (Byerly et al., 1984; DeCoursey and Cherny, 1994) but is distinct in its high sensitivity to temperature. The presence of a temperature-sensitive and voltage-dependent H^+ efflux is confirmed by measuring pH_i using BCECF. The mean conductance is reduced by omitting intracellular ATP, so that ATP may modulate the current activity at least partly. The H^+ conductive pathway would contribute to pH regulation

Address correspondence to Miyuki Kuno, MD, Ph.D., Department of Physiology, Osaka City University Medical School, Abeno-ku, Osaka 545, Japan. Fax: 06-645-2015; E-mail: kunomyk@msic.med.osaka-cu.ac.jp

[1]*Abbreviations used in this paper:* BCECF, 2′,7′-bis-(2-carboxyethyl)-5(and 6)carboxy-fluorescein; BMMC, bone marrow-derived mast cells; E_H, equilibrium potential for H^+; pH_i, intracellular pH; pH_o, extracellular pH; pH_p, the pH of pipette solution; V_{rev}, reversal potential.

of BMMC during metabolic acidosis associated with cell growth, production of large amounts of chemical mediators, or performance of other cellular functions. A preliminary account has been made (Kuno et al., 1995*b*).

MATERIALS AND METHODS

Cells

Bone marrow cells were obtained from the femoral and tibial bones of male, 8–10-wk-old mice (Balb/ca). The mice were killed by an overdose of ether. Pokeweed mitogen–stimulated spleen cell-conditioned medium (PWM-SCM) was prepared as described elsewhere (Nakahata et al., 1982). Briefly, mouse spleen cells were incubated at 37°C in a 95% air–5% CO_2 atmosphere with pokeweed mitogen (1:300 dilution) (GIBCO BRL Products, Gaithersburg, MD) in α-MEM (INC Pharmaceuticals Inc., Irvine, CA) supplemented with 10% FCS (INC Pharmaceuticals Inc.), 10^{-4} M 2-mercaptoethanol, streptomycin (0.1 mg/ml), penicillin (100 U/ml), and amphotericin B (0.25 μg/ml). After 5 d of incubation, the supernatant (PWM-SCM) was filtered with a millipore filter (0.22 μm) and stored at −85°C. Bone marrow cells were plated at 10^6/ml in 35-mm petri dishes and were incubated at 37°C in a 95% air–5% CO_2 mixture. The culture medium contained α-MEM, 10^{-4} M 2-mercaptoethanol, 10% FCS, and 10% PWM-SCM. Half of the medium was changed every week. Cells densely stained with alcian blue (Worthington, 1962) were identified as BMMC. BMMC appeared within 2–4 wk and were maintained for more than 6 months. Cells cultured for more than 4 wk were used in this experiment, because the purity of BMMC was ≥90–95%.

Solutions

The standard pipette solution contained (mM): 150 K-glutamate, 7 $MgCl_2$, 1 EGTA, 1–2 Na_2ATP, and 10 HEPES (pH = 7.3). In some experiments, K-glutamate was replaced by CsCl. In acidic intracellular solutions, pH was buffered with 10 or 120 mM Mes. With 120 mM Mes, K-glutamate or CsCl was reduced to 100 mM to compensate for the osmolality, and the pH was adjusted to 5.5 by 14–20 mM KOH. The pH of the pipette solutions was designated as pH_p. The standard extracellular solution contained: 145 mM NaCl, 5 mM KCl, 1 mM $CaCl_2$, 1 mM $MgCl_2$, 10 mM HEPES, 10 mM glucose, and 0.1% BSA (pH = 7.3). Extracellular solutions were buffered with 10 mM Mes for pH ≤ 6.7 and with 10 mM 2-(cyclohexylamino)ethanesulfonic acid (CHES) for pH ≥ 8.2. NaCl was replaced by KCl to make a K^+-rich (150 mM) solution and by *N*-methyl-D-glucamine (150 mM) to make a NMG^+-rich solution. A low Cl^- solution was prepared by replacing NaCl with Na-isethionate. With 10 mM buffers, the pH was adjusted by KOH (3–8 mM) in the intracellular or K^+-rich external solutions and by NaOH (3–8 mM) in other external solutions.

Recordings

Current signals were recorded from the whole-cell voltage clamp configuration. The reference electrode was an Ag-AgCl wire connected to the bath solution through a Ringer-agar bridge. Pipette resistance ranged between 5 and 15 MΩ. The zero-current potential before formation of the gigaseal was taken as 0 mV. The recording chamber was placed on a heating plate (MT1; Narishige, Tokyo, Japan), and the bath temperature was changed between 24 and 36°C. The current signals were led into a patch-clamp amplifier (EPC7; LIST, Darmstadt, Germany) without series resistance compensation, digitized at 1–4 kHz with an analog–digital converter (MacLab/4; Analogue Digital Instruments, Australia) and stored on a personal computer. Cell capacitance was estimated with capacitive cancellation circuitry on the amplifier (5.3 ± 1.0 pF, n = 142). We started to collect data within 1–2 min after the formation of the whole cell configuration, since the H^+ current appeared within 10–30 s after the rupture of the patch membrane and usually did not further increase at 32–36°C. Leak current was determined from the linear portion of the current-voltage (I-V) relation when either inward or outward current was absent or when the currents were eliminated by the blockers. The inward and outward conductances were obtained from the I-V relation between −110 and −80 mV and between +50 and +100 mV, respectively, after subtraction of the leak current. To obtain the I-V relation, voltage pulses were applied at an interval of 3 min. All data were expressed as mean ± SD. Statistical significance was evaluated with Student's unpaired t test. The goodness of fit of single exponential distribution to the activation kinetics and tail currents was determined by the χ^2 test. In most cases, P values for the fit were greater than 0.95.

Measurements of pH_i by BCECF

Macroscopic pH_i was determined by loading populations of BMMC (3–6 × 10^5 cells/ml) with a pH-sensitive fluorescent dye, 2′,7′-bis-(2-carboxyethyl)-5 (and -6) carboxyfluorescein (BCECF). Cells were incubated with the acetoxymethyl ester form of BCECF (BCECF-AM) (1 μM) for 30 min and then, after washing the dye, with 40 mM NH_4Cl for 15 min at 36°C. Washing cells by ammonium-free solutions rapidly acidified cells (Roos and Boron, 1981). Recovery of pH_i in the acid-loaded cells was measured by a spectrofluorometer (650-60; Hitachi, Tokyo, Japan). The ratio of fluorescences excited at two wavelengths, 490 and 450 nm (bandwidth; 3–5 nm), was obtained at an interval of 1 min. The emission wavelength was 530 nm (bandwidth; 6–10 nm). Calibration of pH_i was carried out by dissipating plasma membrane pH gradient with 10 μM nigericin in a K^+-rich solution with known pH values (Thomas et al., 1979; Grinstein and Furuya, 1988). To eliminate contamination with nigericin (Richmond and Vaughan-Jones, 1993), the cuvette and teflon-coated spin bar were rinsed by ethanol before use. The rate of the pH_i recovery was estimated by differentiating the pH_i recordings.

Substances

A condensed stock solution of Na_2ATP (500 mM) was prepared in 1 M Tris Cl, stored in a freezer, and added to the internal medium before use. Condensed stock solutions of 4,4′-diisothiocyano-2,2′-stilbenedisulphonate (DIDS) and $ZnCl_2$ were dissolved in distilled water. The free concentration of Zn^{2+} was not determined and the concentration described herein is only nominal, since Zn^{2+} forms complexes with anions. Bafilomycin A_1 was prepared in ethanol. The final concentration of ethanol was ≤0.5%. BCECF-AM, CHES and Mes were obtained from Dojindo Laboratories (Kumamoto, Japan), and other chemicals were obtained from Sigma Chemical Co. (St. Louis, MO).

RESULTS

Elevation of Temperature Activates an Outward Current

Fig. 1 *A* illustrates a representative time course of changes in the whole cell current when temperature of the recording chamber was altered (*top*). Upward and downward vertical lines in the bottom trace represent outward and inward currents evoked by voltage ramps (200 mV/s) applied at a holding potential of 0 mV

(*middle*). Heating from 24 to 36°C reversibly and repeatedly activated outward currents both in the K^+-rich (150 mM K^+) and the standard Ringer (5 mM K^+) solutions. Fig. 1, *B* and *C*, show superimposed current-voltage (I-V) relations obtained by the voltage ramps during heating in the K^+-rich (*B*) and the standard Ringer (*C*) solutions.

Temperature-conductance relationships (see MATERIALS AND METHODS) in three cells show that heating from 24 to 36°C gradually increased the outward conductance, although the magnitude varied greatly among cells (Fig. 2 *A*). The inward conductance of these cells remained unchanged or increased only slightly by the heating (Fig. 2 *B*). Fig. 2 *C* summarizes semilogarithmic plots of the outward conductance against temperature in six cells with a linear regression for all data. The conductance was normalized to that measured at 36°C. The factor by which the conductance changes per 10°C elevation (Q_{10}) was 9.9 ± 3.1 (n = 6).

Although the outward current described above was recorded at pH_p (pH of the pipette solution) 7.3, the current larger than 10 pA at the end of a 500-ms voltage pulse of +100 mV was evident only in 7 of 19 cells at 32°C. The current was seen more frequently at lower pH_p. At pH_p 5.5, 80 of 103 cells exhibited the outward current, although the percentage of cells with the current varied among different cell batches from 70 to 92%. The magnitude normalized by cell capacitance was generally much smaller at pH_p 7.3 (2.4 ± 7.3 pA/pF, n = 19) than that at pH_p 5.5 (9.6 ± 9.5 pA/pF, n = 103). At pH_p 5.5, the outward current was detected in some cells even at 24°C and was enhanced by heating with Q_{10} of 6.0 ± 2.6 (n = 9). In later experiments, the heating-activated outward current was analyzed at pH_p 5.5 to optimize the detection of the current unless described otherwise.

Fig. 3 *A* shows a family of currents activated by depolarization pulses in +20-mV increments applied at −40 mV at 32°C. The outward current was characterized by slow activation kinetics at depolarization, differing from the rapidly activating, outwardly rectifying Cl^- current that we reported previously (Kuno et al., 1995*a*). Activation followed a single exponential time course (*thin lines*) after a small delay and was facilitated at more positive potentials. The activation time course was also greatly

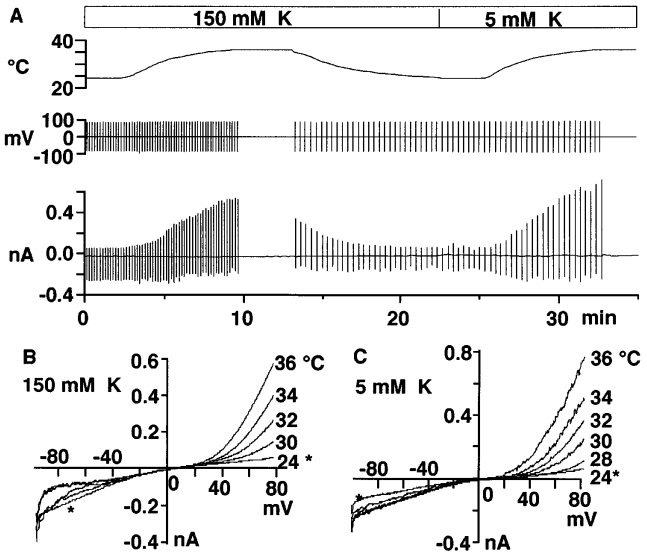

FIGURE 1. Effects of changes in temperature on whole cell current. (*A*) Temperature (*top*), voltage (*middle*), and current (*bottom*) recordings during changes in bath temperature between 24 and 36°C. Vertical lines in the bottom indicate currents associated with voltage ramps applied at 0 mV. The cell was suspended first in the K^+-rich (150 mM) solution and then in the standard (5 mM K) solution (pH_o = 7.3). (*B* and *C*) Current-voltage relations obtained by voltage ramps during heating in 150 and 5 mM K^+ solutions. *Denotes data at 24°C. *A–C* were obtained from the same cell. The pipette contained K-glutamate (pH_p = 7.3).

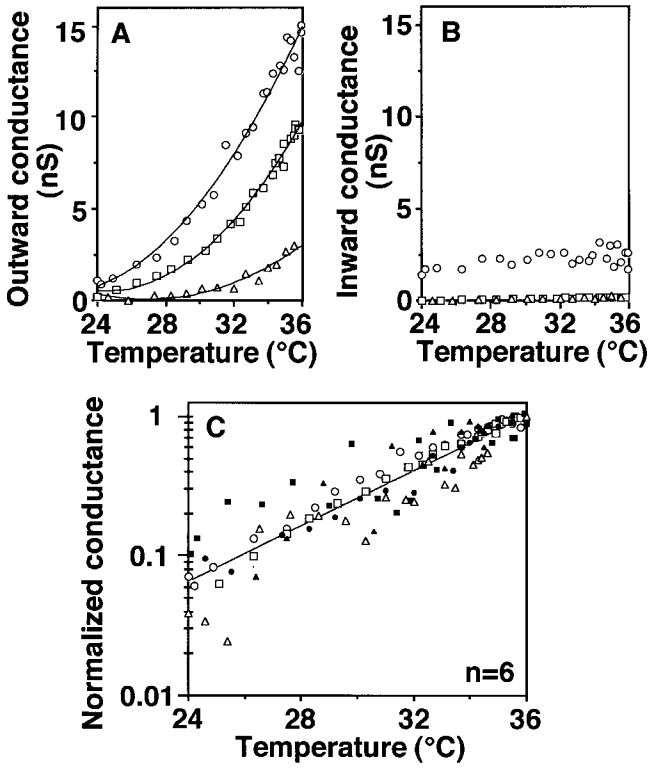

FIGURE 2. Temperature-conductance relationships. (*A* and *B*) Outward (*A*) and inward (*B*) conductances of three cells plotted against temperature. Conductances were estimated from I-V curves obtained by voltage ramps applied at 0 mV, between +50 and +100 mV for outward currents and between −110 and −80 mV for the inward currents. Curves are the second order polynomial fit for data. (*C*) Semilogarithmic plots of the outward conductance against temperature. Data were normalized as the partition of the amplitude at 36°C. Different symbols indicate data from different cells (n = 6). The external solution contained the standard Ringer and the internal solution contained K-glutamate (pH_p/pH_o = 7.3/7.3). The line is a least square's fit for all data.

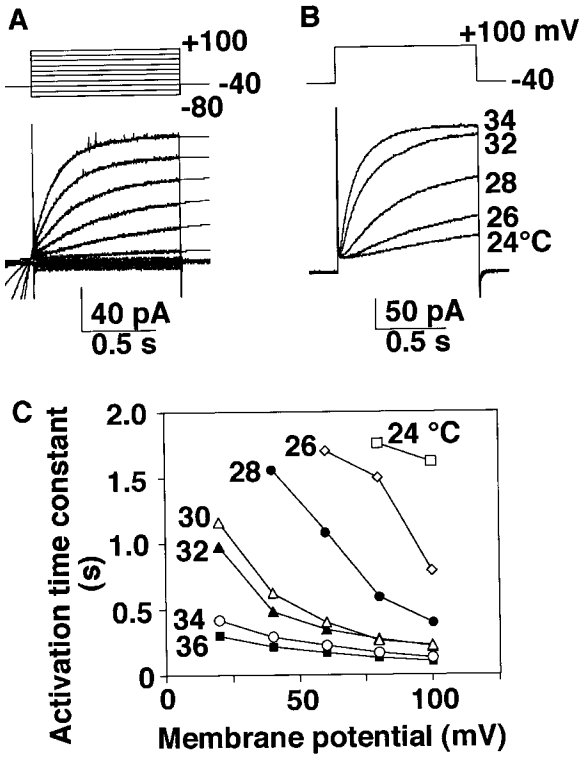

FIGURE 3. Characteristics of heating-activated outward current. (*A*) A family of currents obtained by voltage steps in 20-mV increments applied at −40 mV and superimposed single exponential fits. The currents were recorded at 32°C. (*B*) Outward currents evoked by a depolarization pulse of +100 mV applied at −40 mV when temperature was elevated from 24 to 34°C. (*C*) Activation time constant at different potentials. *B* and *C* are obtained from the same cell. The pH_p/pH_o was 5.5/7.3. The internal buffer was 120 mM Mes.

affected by temperature. Fig. 3 *B* illustrates superimposed outward currents evoked by a depolarizing pulse to +100 mV applied at −40 mV when temperature was elevated from 24 to 34°C in a cell. Relationships between the activation time constant and the membrane potential at different temperatures in this cell indicate that at any given potential the time constant becomes shorter at higher temperatures (Fig. 3 *C*). Similar results were obtained from five cells tested. Further experiments were performed at 32°C, as recordings at 36°C were often unstable.

The Heating-activated Outward Current Is Mediated Mainly by Proton (H^+)

Averaged I-V plots obtained from different cells at three pH_p (5.5–7.3) are presented in Fig. 4 *A*. The pH_o was the same (7.3) in all cases. The currents were measured at the end of 500-ms voltage pulses. The acidic intracellular solutions were buffered either with 10 or 120 mM Mes. Little current was detectable at potentials more negative than 0 mV. Although there was cell-to-cell variability in the potential at which activation occurred, lowering pH_p shifted the voltage dependency to a more negative direction. On the other hand, elevating pH_o from 7.3 to 8.7 reversibly shifted the I-V curves to a more negative direction in all cells tested ($n = 12$) (Fig. 4 *B*). This shift by extracellular alkalization was observed even in cells recorded with the pipette containing CsCl (Fig. 4 *C*). The time course of activation was accelerated by increasing pH_o. At +80 mV with pH_p 5.5, the time constant at pH_o 8.2–8.7 was 327 ± 61 ms ($n = 5$), significantly faster than that at pH_o 7.3 (625 ± 255 ms, $n = 11$; $P < 0.05$).

The outward currents appeared within 10–30 s after the rupture of the patch membrane to form the whole cell configuration with the acidic pipette solutions buffered by either 10 or 120 mM Mes. Thus BMMC seemed to be acidified quickly, probably because of the small cell size (radius; 5.1 ± 0.7 μm, $n = 142$). The current amplitude at the end of a 500-ms voltage pulse of +100 mV at pH_o 5.5 was 8.9 ± 10.0 pA/pF ($n = 63$) with 10

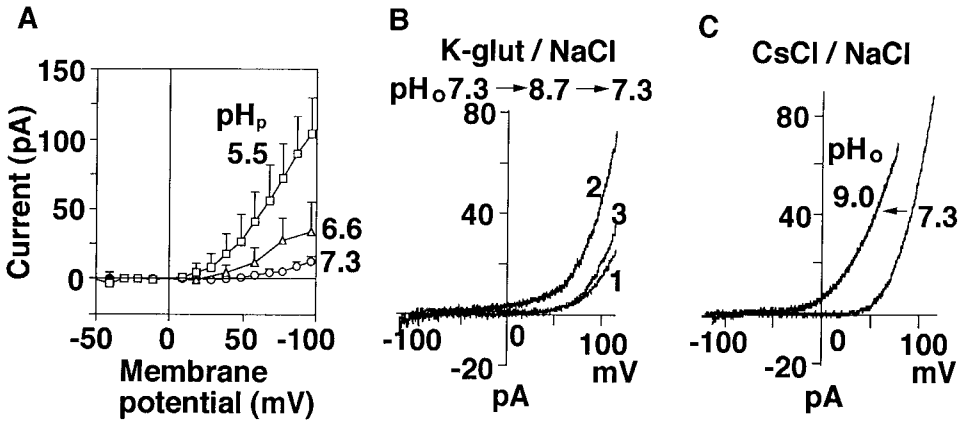

FIGURE 4. Effects of pH_p and pH_o on heating-activated outward current. (*A*) Averaged I-V plots with pH_o 7.3 at pH_p 5.5 (*squares*, $n = 9$), 6.6 (*triangles*, $n = 3$), and 7.3 (*circles*, $n = 7$). The current was measured at the end of 500-ms voltage pulses. The internal buffer (Mes) was 10 mM in seven of nine cells at pH_p 5.5 and 120 mM in two cells at pH_p 5.5 and in three cells at pH_p 6.6. B, I-V relations obtained from voltage ramp applied at 0 mV when the pH_o was changed from 7.3 (*1*) to 8.7 (*2*) and then returned to 7.3 (*3*). The internal medium contained K-glutamate. (*C*) I-V relations recorded with the pipette solution containing CsCl when the pH_o was increased from 7.3 to 9.0. *B* and *C* were obtained from different cells at pH_p 5.5 with 10 mM Mes. Leak current was subtracted. *A–C* were obtained at 32°C.

mM Mes, not significantly different from that with 120 mM Mes (10.8 ± 8.7 pA/pF, n = 40). I-V relations obtained by 500-ms voltage pulses from −100 to +100 mV, and intermittent voltage ramps were not affected by the buffering power. However, when a 1-s depolarizing pulse (+100 mV) was repetitively applied at an interval of 3 s, a gradual rundown of the outward current was observed with 10 mM Mes (by 19.1 ± 18.6% per 10 pulses, n = 16) but not with 120 mM Mes (by −1.5 ± 11.0% per 10 pulses, n = 14). In addition, when the cells were exposed to an 8-s depolarization (+60 mV), the current amplitude gradually increased to a peak and then reduced to 87.0 ± 9.3% (n = 11) of the maximum at the end of the depolarization with 10 mM Mes and 95.2 ± 5.6% (n = 11) with 120 mM Mes. The decline was greater with the lower concentration of Mes ($P < 0.05$). Thus a high buffering power in pipette solutions was needed to maintain the current.

To determine ion species carrying the current, the currents were studied under various experimental conditions. The outward current was observed both when the extracellular Cl^- ($[Cl^-]_o$) was totally replaced by isethionate$^-$ (Fig. 5 *A*) and when the intracellular K^+ was totally replaced by Cs^+ (Fig. 5 *B*). Tail currents at 0 mV after the depolarizations were directed outwardly (*arrow*) and were fit by single exponential curves as in-

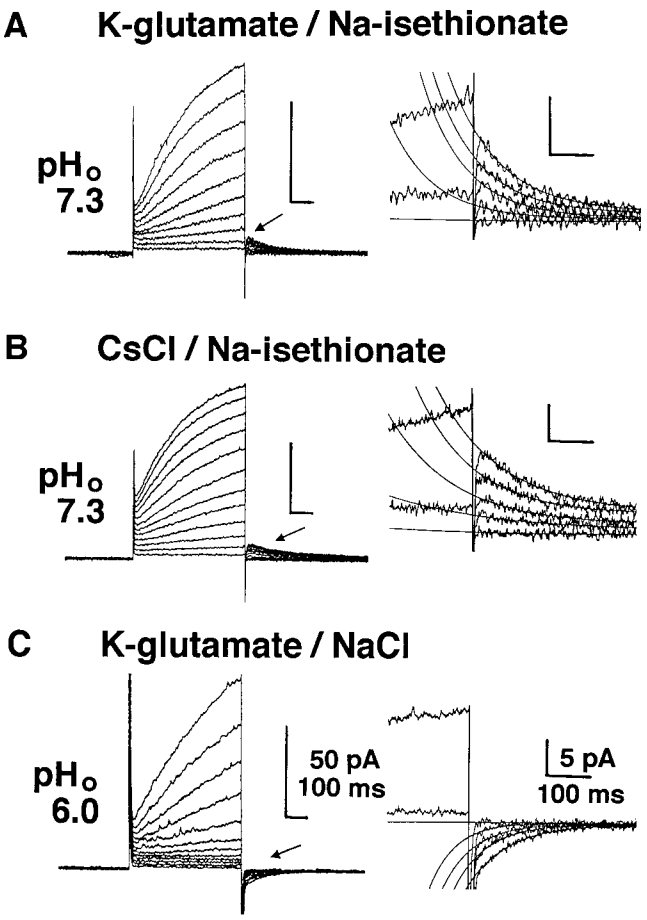

FIGURE 5. Heating-activated outward current recorded in various internal and external solutions. Whole cell currents evoked by voltage pulses up to +100 (*A*) or +120 mV (*B* and *C*) in +10-mV increments at pH_p 5.5 (32°C). The holding potential was 0 mV. The internal solution was buffered with 120 mM Mes. Selected traces of tail currents (*arrows*) were magnified with superimposed single exponential fits (*right*). (*A*) The internal and external media contained K-glutamate and Na-isethionate, respectively. Tail currents induced by prepulse of +10, +30, +50, +70, and +100 mV are superimposed. (*B*) The internal and external media contained CsCl and Na-isethionate. Tail currents with prepulse of +10, +30, +40, +60, and +100 mV are superimposed. (*C*) The internal and external media contained K-glutamate and NaCl. Tail currents at +10, +70, +90, +100, and +120 mV are superimposed. 50 μM of DIDS was added into all external media. pH_o: 7.3 (*A* and *B*) and 6.0 (*C*).

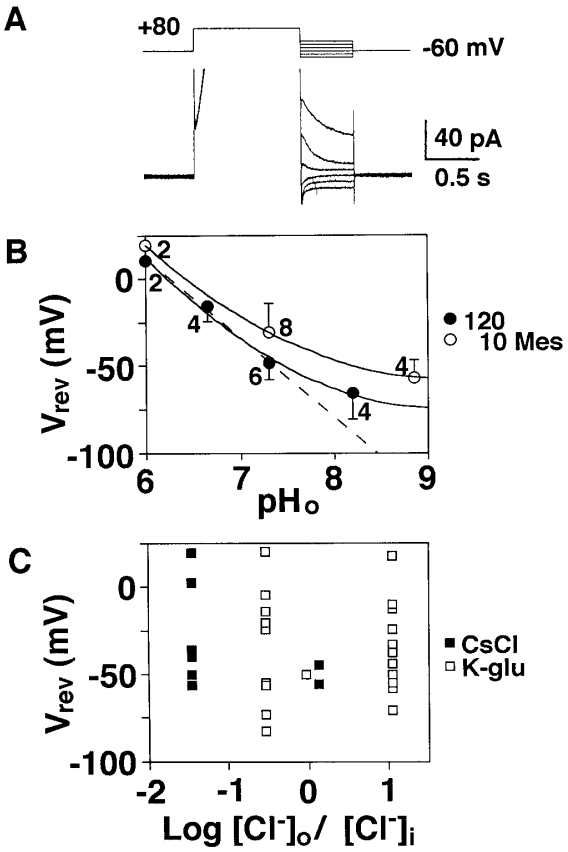

FIGURE 6. Reversal potential of heating-activated outward current. (*A*) Tail currents after a depolarization prepulse (+80 mV) at pH_p 5.5. The outward current evoked by the prepulse is truncated. (*B*) Relationships between pH_o and the reversal potential (V_{rev}) estimated from tail currents following a prepulse of either +80 or +100 mV (1 s). Open and closed circles represent mean and SD of data recorded with 10 and 120 mM Mes. The solid curves are fitted by eye and the dotted line, a linear regression for data at pH_o 6.0, 6.7, and 7.3 with 120 mM Mes. Figures attached with data indicate the number of cells. (*C*) V_{rev} plotted against the ratio between extracellular and intracellular Cl^- concentrations ($[Cl^-]_o/[Cl^-]_i$) on a semilogarithmic scale. Open and closed squares represent data recorded with K-glutamate and CsCl in the internal solution, respectively. *B* and *C* were obtained from the same data. The external medium was same (standard Ringer) except for pH_o.

dicated by superimposed thin lines in the magnified record (*right*). In these recordings, the external medium contained a Cl^- channel blocker, DIDS (50 μM), which blocks the Cl^- current in BMMC (Kuno et al., 1995*a*). Addition of a K^+ channel blocker, Ba^{2+} (1 mM) did not affect the current. When the pH_o was 6.0, the outward current was small in most cells, but sizable currents were observed in a few cells (Fig. 5 *C*). Tail currents in these cells were going inwardly at 0 mV, suggesting that lowering pH_o from 7.3 to 6.0 shifted the reversal potential (V_{rev}) to a more positive level.

The V_{rev} was estimated from the I-V plots for instantaneous tail currents recorded in cells with larger currents. The voltage protocols were made of test pulses after the 1-s prepulse (either +80 or +100 mV) (Fig. 6 *A*). The amplitudes of tail currents at the start of each test pulse were determined from the single exponential fit as shown in Fig. 5. Closed circles in Fig. 6 *B* represent the averaged V_{rev} at pH_p 5.5 recorded with 120 mM Mes in the pipette solutions. The V_{rev} became more negative in alkaline media. The dashed line represents a linear regression for data at pH_o 6.0–7.3 with 120 mM Mes, having a slope of 45.5 mV per ΔpH_o of 1. Data at higher pH_o deviated from the regression line. Departures from the line were more prominent with 10 mM Mes (*open circles*). When the V_{rev} was replotted against the ratio between extracellular and intracellular Cl^- concentrations ($[Cl^-]_o$ and $[Cl^-]_i$) on a semilogarithmic scale (Fig. 6 *C*), the V_{rev} did not depend on the Cl^- gradient. Open and closed squares represent data recorded with pipette containing K-glutamate and CsCl, respectively, showing that the V_{rev} did not depend on the K^+ concentration. These results suggest that the heating-activated outward current is carried primarily by H^+ (equivalents).

Effects of Zinc, Bafilomycin A_1, and ATP on the H^+ Current

A blocker for H^+ conductances, $ZnCl_2$ (0.25–0.5 mM), reversibly suppressed the outward current to 10 ± 10.3% (n = 8) of the controls (Fig. 7). On the other hand, the current amplitude in the presence of bafilomycin A_1 (100 nM), a potent and selective inhibitor for the H^+-ATPase (Bowman et al., 1988), was 47.1 ± 37.5 pA at the end of a 500-ms pulse of 100 mV (n = 20), not significantly different from the controls (56.2 ± 41.0 pA; n = 22). It seems that the H^+ current is not mediated via an electrogenic vacuolar type H^+-ATPase.

As high sensitivity to temperature implicated that a high activation energy would be involved in the current activity, we examined the effects of intracellular ATP on the H^+ current. Fig. 8 shows I-V plots from cells recorded with ATP-containing (*A*) and ATP-omitting (*B*) pipette solutions. The data were obtained from the same batch of cells, to avoid batch-to-batch variation. The H^+ conductance recorded without ATP was 104 ± 54 pS/pF (n = 10), significantly smaller than that observed with ATP (216 ± 143 pS/pF; n = 10) ($P < 0.05$). Thus, ATP might be involved in potentiation of the H^+ current.

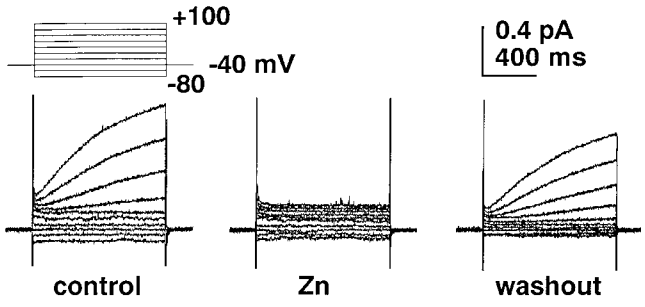

FIGURE 7. Blockade of H^+ current by Zn^{2+}. Whole cell currents evoked by voltage pulses from −80 to +100 mV in 20-mV steps applied at −40 mV at 32°C (pH_p/pH_o = 5.5/7.3). The outward current was reversibly inhibited by 0.25 mM $ZnCl_2$. The internal solution contained K-glutamate and 120 mM Mes and the external solution, Na-isethionate.

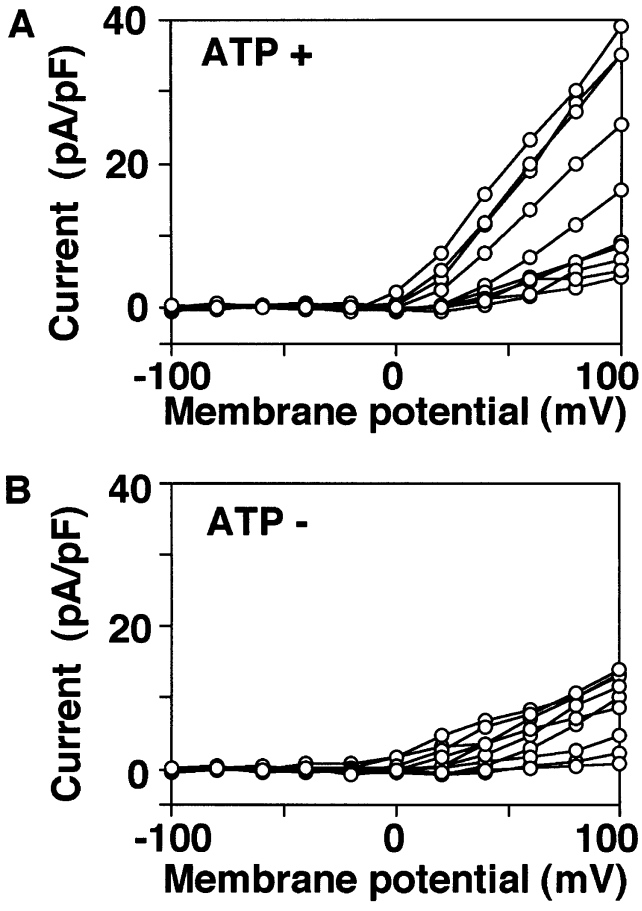

FIGURE 8. Effects of intracellular ATP on H^+ current. I-V plots normalized by the cell capacitance for each 10 cells recorded with ATP (1 mM)-containing (*A*) and ATP-omitting (*B*) intracellular solutions. The current amplitude was measured at the end of 500-ms voltage pulses applied at −40 mV at 32°C (pH_p/pH_o = 5.5/7.3). The pipette solution was buffered with 120 mM Mes.

Measurements of Macroscopic pH_i Recovery in Acid-loaded Cells

To assess the role of the H^+ conductance in regulation of pH_i, pH_i recovery from acid-load in populations of BMMC was measured using a fluorescent pH-sensitive dye, BCECF (Fig. 9). Washing cells preincubated with NH_4Cl by ammonium-free solutions induced intracellular acidification (Roos and Boron, 1981), followed by a pH_i recovery in an Na^+-free K^+-rich solution at 36°C (Fig. 9, *closed circles*) (see MATERIALS AND METHODS). Although the time course and the resultant pH level at ~20 min differed among preparations, the pH_i recovery was characterized by an initial rapid phase within 5–10 min. The Na^+-independent pH_i recovery was reduced at 24°C (Fig. 9 *A*). In an Na^+-free NMG^+-rich medium (Fig. 9 *B*), which would hyperpolarize cells, the pH_i recovery was greatly inhibited, suggesting that depolarization is required for the rapid H^+ efflux. Addition of 0.5 mM $ZnCl_2$ attenuated the pH_i recovery (Fig. 9 *C*), but bafilomycin A_1 (100 nM) did not (Fig. 9 *D*).

The inhibitory effect of low temperature and Zn^{2+} seemed to be more prominent during the initial phase of pH_i recovery. The rate of the pH_i change per time (ΔpH/min), obtained by differentiating the pH_i recordings, was attenuated by lowering temperature (*open circles*) and was greatly inhibited by 0.5 mM Zn^{2+} (*squares*) (Fig. 10). The rate at 0 min was 0.049 ± 0.029 pH U/min (n = 7) at 24°C, 0.010 ± 0.010 pH U/min (n = 5) in the presence of Zn^{2+}, and 0.110 ± 0.068 pH U/min (n = 12) in their controls. These results support an idea that a temperature- and Zn^{2+}-sensitive H^+ conductive pathway is responsible for a rapid pH_i regulation during intracellular acidification. The slow pH_i recovery remaining in the presence of Zn^{2+} may be mediated by unidentified H^+ efflux mechanisms other than the H^+ conductance.

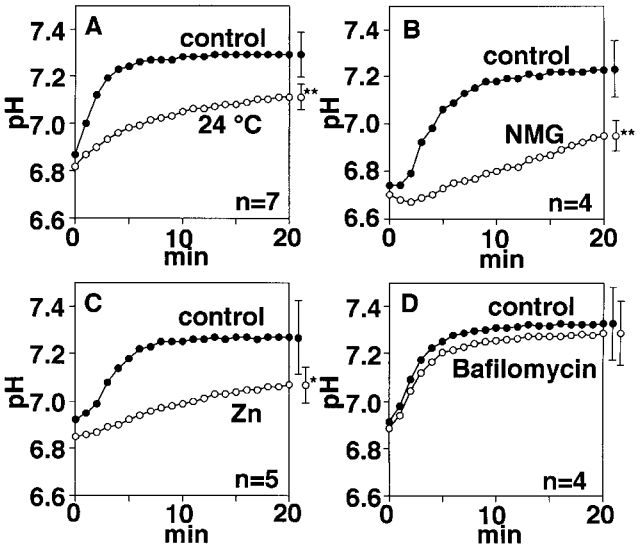

FIGURE 9. Macroscopic measurements of pH_i recovery in acid-loaded cells. Populations of cells were loaded with BCECF-AM and incubated in the presence of 40 mM NH_4Cl for 15 min. The ordinate indicates averaged pH_i in these cells after washings with ammonium-free solutions. Closed circles in *A–D* represent data recorded at 36°C in the Na^+-free, K^+-rich solution (*control*). Open circles represent averaged pH_i at 24°C in the K^+-rich medium (*A*, n = 7), in the Na^+-free NMG^+-rich solution (*B*, n = 4), in the presence of 0.5 mM $ZnCl_2$ (*C*, n = 5), and 100 nM bafilomycin A_1 (*D*, n = 4) in the K^+-rich solution. Symbols with bars at right are mean ± SD for data at 20 min; * and ** indicate $P < 0.05$ and $P < 0.01$, respectively. Changes in pH_i in *B–C* were measured at 36°C.

DISCUSSION

A Temperature-sensitive H^+ Conductance

We recently reported that an electrophysiological profile of BMMC was heterogeneous at room temperature, such that an inwardly rectifying K^+ current and an outwardly rectifying Cl^- current were exhibited in subpopulations (Kuno et al., 1995*a*). The present study described a voltage-activated outward current which was negligible or small at room temperature but was remarkably augmented by heating up to 36°C. H^+ (equivalents) was suggested to be an ion species primarily responsible for the heating-activated current from several lines of evidence. First, either a decrease in pH_p or an increase in pH_o increased the current amplitude and shifted the activation voltage to more negative poten-

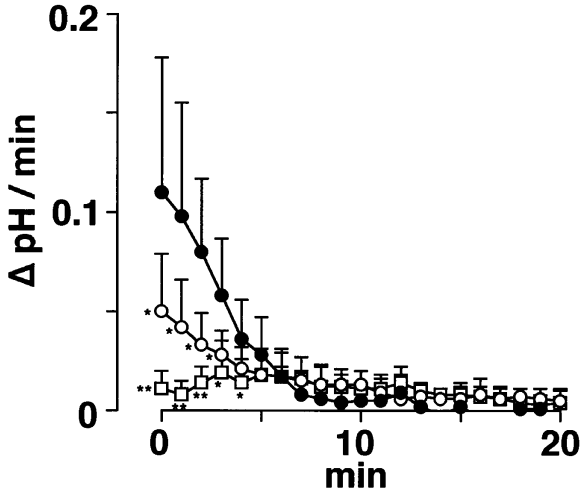

FIGURE 10. The rate of pH_i recovery from acidification. The rate of pH_i change per time (ΔpH/min) during the recovery from acidification was obtained by differentiating individual pH_i recordings averaged in Fig. 9, *A* and *C*. Open circles, squares, and closed circles represent mean and SD of the ΔpH/min at 24°C (n = 7) in the presence of 0.5 mM Zn^{2+} (n = 5) and their controls (n = 12). The acid-loaded cells were suspended in the K^+-rich medium. The pH_i in the Zn^{2+}-containing or control solutions was measured at 36°C.

tials. Second, the current was observed even when the extracellular Cl^- was replaced by an impermeable anion, isethionate$^-$, and when the intracellular K^+ was replaced by Cs^+. Third, the V_{rev} was dependent on the H^+ gradient but was unaffected by the substitution of other major ion constituents (Cl^-, K^+, Na^+). Fourth, the current was not inhibited by K^+ or Cl^- channel blockers (Ba^{2+} and DIDS) but by Zn^{2+}, a blocker for voltage-activated H^+ currents (Kapus et al., 1993).

The H^+ current in BMMC shares major properties of that in other cell types (voltage- and time-dependent activation, outward rectification, sensitivity to both pH_o and pH_i, and a blockage by heavy metals) but is distinct in its high sensitivity to temperature. Although H^+ currents of snail neurons have a stronger temperature sensitivity than K^+ currents over a temperature range of 10–25°C (Byerly and Suen, 1989), sizable H^+ currents were described in many mammalian cells at room temperature. It is possible that the H^+ conductive pathway comprises a diverse family of related types whose characteristics may be tissue specific and that activation mechanisms of the H^+ current in BMMC may differ from that in other cells. However, literature on the sensitivity of voltage-activated H^+ currents to temperature is too scarce to draw this conclusion at this moment.

Characteristics of the H^+ Current in BMMC

Although H^+ (equivalents) was estimated to be a primary constituent for the heating-activated outward current in BMMC, the V_{rev} deviated from the E_H predicted by the Nernst formula especially at high pH_o, even when the current was recorded with a high buffering power (120 mM Mes) in the pipette solutions. Prepulse protocols consisted of different durations (0.5–4 s), and the holding potentials (0 and −60 mV) did not affect the result. Similar deviation of the V_{rev} was often described with H^+ currents in other cell types (Mahaut-Smith, 1989; DeCoursey, 1991; Bernheim et al., 1993; Demaurex et al., 1993; Kapus et al., 1993), and some intrinsic buffering action or diffusion limitation suggested a deviation from the nominal pH_p value (DeCoursey, 1991; Kapus et al., 1993; Holevinsky et al., 1994). The deviation of the V_{rev} from the expected value was greater with 10 mM Mes, although the buffering power of the pipette solutions (10 or 120 mM Mes) did not significantly affect the current amplitude obtained by 500-ms step pulses or ramp pulses from −100 to +100 mV. This may result from depletion of the intracellular H^+ concentration during repetitive prepulses. Decline of voltage-activated H^+ currents during long-lasting depolarization has been reported (Barish and Baud, 1984; DeCoursey, 1991; Demaurex et al., 1993; Kapus et al., 1993) and is explained by depletion of H^+ currents caused by preceding H^+ efflux (Kapus et al., 1993). It seems that a high intracellular buffering power is needed to maintain the H^+ current during long-lasting or repetitive depolarization.

So far, direct electrophysiological evidence that the H^+ currents are mediated by channels is not available (Lukacs et al., 1993), as the current noise is small and single channel current is hardly seen even in isolated patches (DeCoursey and Cherny, 1995). Noise analysis estimated that the single channel conductance is <10 fS (Byerly and Suen, 1989; Bernheim et al., 1993; DeCoursey and Cherny, 1993). In isolated patches of alveolar epithelial cells, H^+ permeation mechanisms through voltage-activated H^+ channels suggest a difference from those permeated through water-filled ion channels (DeCoursey and Cherny, 1995). The current noise was small and was not augmented by depolarizations in BMMC as well. Little noise, high sensitivity to temperature, and a slow activation rate raises a possibility that H^+-conducting molecules in BMMC may be intermediate between channel and carrier proteins, although this is only conjecture.

Effects of ATP on the H^+ Current

A vacuolar type H^+-ATPase is known as an electrogenic H^+ transport system. The H^+-ATPase, generally localized in membranes of intracellular organelles, is found in the plasma membrane of osteoclasts (Väänänen et al., 1990) and macrophages (Swallow et al., 1988). The F_o component of the H^+-ATPase in osteoclasts forms a channel protein to secrete H^+ (Junge, 1989). As osteoclasts generate from bone marrow cells, it is conceivable that BMMC would possess a similar plasmalemmal H^+-ATPase. However, the H^+ current in BMMC cannot be well explained by a vacuolar type H^+-ATPase for the following reasons: First, the current is recorded in some cells even when ATP is omitted from the intracellular milieu. Second, bafilomycin A_1, a selective and potent blocker for the vacuolar type H^+-ATPase (Bowman et al., 1988), does not block the current. Third, immunohistochemical studies documented that the antibody for the vacuolar H^+-ATPase labels osteoclasts but not other cell types of bone marrow (Väänänen et al., 1990). Fourth, the ATPase can pump H^+ against a 10,000-fold uphill concentration gradient (Heldrich et al., 1989), but only outward currents are activated at potentials positive to E_H in BMMC. On this basis and together with the electrophysiological properties (steep voltage-dependence, gating kinetics, the V_{rev}), the H^+-ATPase is unlikely to mediate the H^+ current.

In many cell types, H^+ currents are recorded in the absence of ATP (Byerly and Suen, 1989; DeCoursey, 1991; DeCoursey and Cherny, 1993; Kapus et al., 1993), and a dependency on ATP has not been described. Although the H^+ current was activated in some BMMC even without ATP, the current amplitude was smaller

than that in the presence of ATP. Thus ATP may enhance the current activity either directly or indirectly: the H^+ currents are reported to be amplified by cytoplasmic factors, such as arachidonate (Decoursey and Cherny, 1993), an elevation of intracellular Ca^{2+} (Holevinsky et al., 1994) or phorbol esters (Henderson et al., 1988; Nanda and Grinstein, 1991; Kapus et al, 1992). A direct action of ATP on the molecule mediating the H^+ conductance is an alternative explanation for the ATP dependency. The mechanisms responsible for enhancement by ATP remain to be clarified.

Implications of the H^+ Current in BMMC Functions

Measurements of pH_i using BCECF provide evidence that the H^+ conductive pathway is indeed responsible for the rapid pH_i recovery from acid-load in BMMC, although other unidentified mechanisms may be involved in the slowly developed pH_i recovery. The current amplitude (9.3 ± 9.8 pA/pF at +100 mV and 32°C with pH_p/pH_o of 5.5/7.3) of BMMC is smaller than that in some phagocytes but is roughly comparable to that reported in various cell types (DeCoursey and Cherny, 1994). It is conceivable that metabolic acidosis accompanies cell growth of BMMC as reported in other cell types (Gerson and Kiefer, 1982; Grinstein and Dixon, 1989). Otherwise, maintenance of pH_i may be challenged by releasing large quantities of chemical mediators during anaphylactic actions or in bacterial infection (Echtenacher et al., 1996; Malaviya et al., 1996). The H^+ efflux mechanism dissipates metabolic acids generated during these cellular activities (Lukacs et al., 1993). In addition, many mast cell activities are pH dependent: for example, exocytosis is influenced by pH_i (Alfonso et al., 1994), and enzymes, such as chimases, are strongly pH dependent (McEuen et al., 1995). Thus the H^+ conductance may play a significant role in pH_i regulation of mast cells in various functional states, as in other cells (Hoffman and Simonsen, 1989).

Electrophysiological studies are often conducted at room temperature, which may cause one to overlook the H^+ current. Our results imply that H^+ conductive pathways are expected to exist more widely.

We thank Dr. Matsuura for critically reading the manuscript.

This work was supported by the grants from The Ministry of Education, Science, Culture, Japan and from The Naito Foundation, The Ichiro Kanehara Foundation and The Hoansha Foundation.

Original version received 31 October 1996 and accepted version received 18 March 1997.

REFERENCES

Alfonso, A., M.A. Botana, M.R. Vieytes, M.C. Louzao, and L.M. Botana. 1994. Effect of signal transduction pathways on the action of thapsigargin on rat mast cells: crosstalks between cellular signaling and cytosolic pH. *Biochem. Pharmacol.* 47:1813–1820.

Barish, M.E., and C. Baud. 1984. A voltage-gated hydrogen ion current in the oocyte membrane of the axolotl *Ambystoma. J. Physiol. (Lond.).* 352:243–263.

Bernheim, L., R.M. Krause, A. Baroffio, M. Hamann, A. Kaelin, and C.-R. Bader. 1993. A voltage-dependent proton current in cultured human skeletal muscle myotubes. *J. Physiol. (Lond.).* 470: 313–333.

Bowman, E.J., A. Siebers, and K. Altendorf. 1988. Bafilomycins: a class of inhibitors of membrane ATPases from microorganisms, animal cells, and plant cells. *Proc. Natl. Acad. Sci. USA.* 85:7972–7976.

Byerly, L., R. Meech, and W. Moody, Jr. 1984. Rapidly activating hydrogen ion currents in perfused neurones of the snail, *Lymnaea Stagnalis. J. Physiol. (Lond.).* 351:199–216.

Byerly, L., and Y. Suen. 1989. Characterization of proton currents in neurones of the snail, *Lymnaea Stagnalis. J. Physiol. (Lond.).* 413: 75–89.

DeCoursey, T.E. 1991. Hydrogen ion currents in rat alveolar epithelial cells. *Biophys. J.* 60:1243–1253.

DeCoursey, T.E., and V.V. Cherny. 1993. Potential, pH, and arachidonate gate hydrogen ion currents in human neutrophils. *Biophys. J.* 65:1590–1598.

DeCoursey, T.E., and V.V. Cherny. 1994. Voltage-activated hydrogen ion currents. *J. Membr. Biol.* 141:203–223.

DeCoursey, T.E., and V.V. Cherny. 1995. Voltage-activated proton currents in membrane patches of rat alveolar epithelial cells. *J. Physiol. (Lond.).* 489:299–307.

Demaurex, N., S. Grinstein, M. Jaconi, W. Schlegel, D.P. Lew, and K.-H. Krause. 1993. Proton currents in human granulocytes: regulation by membrane potential and intracellular pH. *J. Physiol. (Lond.).* 466:329–344.

Echtenacher, B., D.N. Männel, and L. Hültner. 1996. Critical protective role of mast cells in a model of acute septic peritonitis. *Nature (Lond.).* 381:75–77.

Gerson, D.F., and H. Kiefer. 1982. High intracellular pH accompanies mitotic activity in murine lymphocytes. *J. Cell Physiol.* 112:1–4.

Grinstein, S., and W. Furuya. 1988. Assessment of Na^+-H^+ exchange activity in phagosomal membranes of human neutrophils. *Am. J. Physiol.* 254:C272–C285.

Grinstein, S., and S.J. Dixon. 1989. Ion transport, membrane potential, and cytoplasmic pH in lymphocytes: changes during activation. *Physiol. Rev.* 69:417–481.

Heldrich, R., A. Kurkdjian, J. Guern, and U.I. Flügge. 1989. Comparative studies on the electrical properties of the H^+ translocating ATPase and pyrophosphatase of the vacuolar-lysosomal compartment. *EMBO (Eur. Mol. Biol. Organ.) J.* 8:2835–2841.

Henderson, L.M., J.B. Chappell, and O.T.G. Jones. 1988. Internal pH changes associated with the activity of NADPH oxidase of human neutrophils: further evidence for the presence of an H^+ conducting channel. *Biochem. J.* 251:563–567.

Hoffmann, E.K., and L.O. Simonsen. 1989. Membrane mechanisms in volume and pH regulation in vertebrate cells. *Physiol. Rev.* 69: 315–382.

Holevinsky, K.O., F. Jow, and D.J. Nelson. 1994. Elevation in intra-

cellular calcium activates both chloride and proton currents in human macrophages. *J. Membr. Biol.* 140:13–30.

Ihle, J.N., J. Keller, S. Oroszlan, L.E. Henderson, T.D. Copeland, F. Fitch, M.B. Prystowsky, E. Goldwasser, J.W. Schrader, E. Palaszynski, M. Dy, and B. Lebel. 1983. Biological properties of homogeneous interleukin 3. I. Demonstration of WEHI-3 growth factor activity, mast cell growth factor activity, P cell-stimulating factor activity, colony stimulating factor activity, and histamine-producing cell-stimulating factor activity. *J. Immunol.* 131:282–287.

Junge, W. 1989. Protons, the thylakoid membrane, and the chloroplast ATP synthase. *Ann. NY Acad. Sci.* 574:268–285.

Kapus, A., R. Romanek, A.Y. Qu, O.D. Rotstein, and S. Grinstein. 1993. A pH-sensitive and voltage-dependent proton conductance in the plasma membrane of macrophages. *J. Gen. Physiol.* 102: 729–760.

Kapus, A., K. Szaszi, and E. Ligeti. 1992. Phorbol 12-myristate 13-acetate activates an electrogenic H^+-conducting pathway in the membrane of neutrophils. *Biochem. J.* 281:697–701.

Krause, R.M., L. Bernheim, and C.-R. Bader. 1993. Human skeletal muscle has a voltage-gated proton current. *Neuromusc. Disord.* 3: 407–411.

Kuno, M., T. Shibata, J. Kawawaki, and I. Kyogoku. 1995*a*. A heterogeneous electrophysiological profile of bone marrow-derived mast cells. *J. Membr. Biol.* 143:115–122.

Kuno, M., T. Shibata, J. Kawawaki, I. Kyogoku, and F. Nakamura. 1995*b*. Temperature-dependent outwardly rectifying currents in bone marrow-derived mast cells. *Jpn. J. Physiol.* 45:S28 (Abstr.).

Lukacs, G.L., A. Kapus, A. Nanda, R. Romanek, and S. Grinstein. 1993. Proton conductance of the plasma membrane: properties, regulation, and functional role. *Am. J. Physiol.* 265:C3–14.

Malaviya, R., T. Ikeda, E. Ross, and S.N. Abraham. 1996. Mast cell modulation of neutrophil influx and bacterial clearance at sites of infection through TNF-α. *Nature (Lond.).* 381:77–80.

Mahaut-Smith, M.P. 1989. Separation of hydrogen ion currents in intact molluscan neurones. *J. Exp. Biol.* 145:439–454.

McEuen, A.R., B. Sharma, and A.F. Walls. 1995. Regulation of the activity of human chymase during storage and release from mast cells: the contribution of inorganic cations, pH, heparin and histamine. *Biochem. Biophys. Acta.* 1267:115–121.

Nakahata, T., S.S. Spicer, J.R. Cantey, and M. Ogawa. 1982. Clonal assay of mouse mast cell colonies in methylcellulose culture. *Blood.* 60:352–361.

Nakano, T., T. Sonoda, C. Hayashi, A. Yamatodani, Y. Kanayama, T. Yamamura, H. Asai, T. Yonezawa, Y. Kitamura, and S.J. Galli. 1985. Fate of bone marrow-derived cultured mast cells after intracutaneous, intraperitoneal and intravenous transfer into genetically mast cell-deficient W/W^V mice: evidence that cultured mast cells can give rise to both connective tissue type and mucosal mast cells. *J. Exp. Med.* 162:1025–1043.

Nanda, A., and S. Grinstein. 1991. Protein kinase C activates an H^+ (equivalent) conductance in the plasma membrane of human neutrophils. *Proc. Natl. Acad. Sci. USA.* 88:10816–10820.

Nordström, T., O.D. Rotstein, R. Romanek, S. Asotra, J.N.M. Heersche, M.F. Manolson, G.F. Brisseau, and S. Grinstein. 1995. Regulation of cytoplasmic pH in osteoclasts: contribution of proton pumps and a proton-selective conductance. *J. Biol. Chem.* 270: 2203–2212.

Razin, E., J.N. Ihle, D. Seldin, J.-M. Mencia-Huerta, H.R. Katz, P.A. Leblanc, A. Hein, J.P. Caulfield, K.F. Austen, and R.L. Stevens. 1984. Interleukin 3: a differentiation and growth factor for the mouse mast cell that contains chondroitin sulfate E proteoglycan. *J. Immunol.* 132:1479–1486.

Richmond, P., and R.D. Vaughan-Jones. 1993. K^+-H^+ exchange in isolated carotid body type-1 cells of the neonatal rat is caused by nigericin contamination. *J. Physiol. (Lond.).* 467:277.

Roos, A., and W.F. Boron. 1981. Intracellular pH. *Physiol. Rev.* 61: 296–434.

Swallow, C.J., S. Grinstein, and O.D. Rotstein. 1988. Cytoplasmic pH regulation in macrophages by an ATP-dependent and N-N′-Dicyclohexylcarbodiimide-sensitive mechanisms: possible involvement of a plasma membrane proton pump. *J. Biol. Chem.* 263: 19558–19563.

Thomas, J.A., R.N. Buchsbaum, A. Zimniak, and E. Racker. 1979. Intracellular pH measurements in Ehrlich ascites tumor cells utilizing spectroscopic probes generated in situ. *Biochemistry.* 18: 2210–2218.

Thomas, R.C., and R.W. Meech. 1982. Hydrogen ion currents and intracellular pH in depolarized voltage-clamped snail neurons. *Nature (Lond.).* 299:826–828.

Väänänen, H.K., E.-K. Karhukorpi, K. Sundquist, B. Wallmark, I. Roininen, T. Hentunen, J. Tuukkanen, and P. Lakkakorpi. 1990. Evidence for the presence of a proton pump of the vacuolar H^+-ATPase type in the ruffled borders of osteoclasts. *J. Cell Biol.* 111: 1305–1311.

Worthington, W.C., Jr. 1962. Dual staining of mast cell cytoplasmic constitution by alcian blue and safranin. *J. Histochem. Cytochem.* 10:503.